UDK 621.793.7:621.643.2-034.14
Original scientific article/Izvirni znanstveni članek

ISSN 1580-2949
MTAEC9, 55(3)337(2021)

COLD-SPRAYED Al-COMPOSITE COATINGS ON S135 DRILL-PIPE STEEL

HLADNO NAPRŠENA Al KOMPOZITNA PREVLEKA NA CEVI ZA VRTANJE IZ JEKLA S135

Dongli Lv[1,2*], Kai Yang[1]

[1]School of New Energy and Materials, Southwest Petroleum University, Chengdu 610500, China
[2]School of Oil and Natural Gas Engineering, Southwest Petroleum University, Chengdu 610500, China

Prejem rokopisa – received: 2020-05-25; sprejem za objavo – accepted for publication: 2021-01-21

doi:10.17222/mit.2020.089

Nine kinds of Al-composite coatings were cold sprayed on the S135 steel. The mechanical properties and microstructures of the coatings were analyzed and the corrosion behavior of the coatings was studied. The surface morphology of the coatings was observed. The porosity of the nine coatings was less than 1.52 %. A proper increase in the Zn powder could reduce the porosity. The thickness of a coating could be increased with an increase in Al_2O_3 and Zn. The hardness of a coating increased obviously after adding Al_2O_3. The friction coefficient of a coating decreased with the increase in Zn and Al_2O_3. The corrosion rate of the coatings decreased with an increase in Al and Al_2O_3.

Keywords: S135, drill-pipe steel, cold-sprayed, Al-composite coatings

Avtorji so s postopkom hladnega naprševanja na jeklene cevi (podaljške) za vrtanje nafte izdelali devet vrst prevlek na osnovi Al kompozitov. Jeklo za cevi je bilo tipa S135. Določili so mehanske lastnosti, mikrostrukturo in korozijske lastnosti izdelanih kompozitnih prevlek ter opazovali morfologijo površine prevlek. Poroznost vseh devetih prevlek je bila manjša od 1,52 % in se je zmanjševala z dodatkom Zn prahu, debelina prevlek pa se je povečevala s povečevanjem vsebnosti Al_2O_3 in Zn. Trdota prevlek je očitno naraščala s povečevanjem dodatka Al_2O_3, medtem ko se je koeficient trenja prevlek zmanjšal s povečevanjem vsebnosti Zn in Al_2O_3. Korozijska hitrost prevlek se je zmanjšala s povečevanjem vsebnosti Al in Al_2O_3.

Ključne besede: S135, jeklena cev (podaljšek) za vrtanje, hladno naprševanje, kompozitne prevleke na osnovi aluminija

1 INTRODUCTION

With a rapid development of modern industry, the demand for oil resources is increasing rapidly. With the expansion of the oil and gas production scope and increase in the production depth, complex oil and gas fields have been put into development. In this case, the exploitation of oil and gas fields is increasingly difficult and its impact on the environment is increasingly serious. The S135 drill-pipe steel is widely used as a drill-pipe material due to its excellent mechanical properties.[1] In recent years, the incidence of drill-pipe failure accidents has been very high, and the losses caused by drill-pipe failures have also increased significantly.[2,3] It is necessary to find a surface treatment method to improve the surface properties of the material while retaining the excellent mechanical properties of the S135 drill-pipe steel.[4] It is an important way of protecting the substrate from corrosion, using a coating to protect the substrate surface and prevent the corrosive medium from reaching the substrate. Organic coating, inorganic coating and metal coating are the main methods of the coating-protection technology. Because of its obvious protective effect, practical and economic advantages, it has been widely used in the steel-structure protection.[5]

*Corresponding author's e-mail:
lvl393@163.com (Dongli Lv)

A protective coating with excellent corrosion resistance and wear resistance can be prepared with thermal spraying or enamel technology. It has been widely used and developed because of its mature technology, convenient preparation and flexible application, but there are inevitably many defects.[6–8] Cold spraying is a technology, during which metal particles hit the substrate surface at a high speed and form a dense coating on the substrate surface. Compared with thermal spraying, cold spraying accelerates the movement of powder particles due to compressed gas, and particles hit the surface of the substrate with their kinetic energy. After collision, plastic deformation occurs, which promotes the deposition of the coating and its bonding with the substrate. Cold spraying does not only create non-oxidized metal deposits in the atmosphere, but also avoids a thermal impact on the substrate. Cold spraying has a broad application prospect in the corrosion protection, preparation of high-conductivity coatings, repair of damaged metal components and manufacture of metal additives.[9–12]

A cold-sprayed Al coating is a kind of anode coating and a good protective material. It can effectively insulate a corrosive medium, prevent it from contacting the steel substrate and prevent corrosion. With respect to electrochemical protection, Zn has a better protection effect than Al, while in terms of electrochemical stability, Al has a better effect than Zn. At the same time, it can be

Table 1: Chemical composition of S135 drill-pipe steel (*w*/%)

C	Si	Mn	S	P	Ni	Cr	Mo	Ti	Cu	Fe
0.28	0.25	0.64	0.004	0.008	0.29	0.98	0.42	0.009	0.02	balance

Table 2: Compositions of the nine Al-composite coatings (*w*/%)

1# Al-80Zn	2# Al-70Zn	3# Al-60Zn	4# Al-10Al_2O_3	5# Al-20Al_2O_3
Al – 80 % Zn	Al – 70 % Zn	Al – 60 % Zn	Al – 10 % Al_2O_3	Al – 20 % Al_2O_3
6# Al-30Al_2O_3	7# Al-60Zn-10Al_2O_3	8# Al-40Zn-15Al_2O_3	9# Al-25Zn-20Al_2O_3	
Al – 30 % Al_2O_3	Al – 60% Zn – 10 % Al_2O_3	Al – 40 % Zn – 15 % Al_2O_3	Al – 25 % Zn – 20 % Al_2O_3	

found that an Al-Zn composite coating is a better material combining the excellent cathodic protection of Zn and the excellent chemical stability of Al.[13–15] However, the hardness of an Al-Zn coating is relatively low. The effect of the hard-phase Al_2O_3 content on the deposition rate and coating performance of a cold-spray Al-Al_2O_3 coating was analyzed. It was found that with the addition of Al_2O_3, the deposition efficiency of the coating was increased by 20–30 %, the porosity was reduced by 1–7 %, the bonding strength was increased by 40–80 MPa and the quality of the coating was improved.[16,17]

In this article, Al-composite coatings with different composition ratios were prepared with cold spraying, and the microstructure characteristics of the coatings were studied and analyzed. The electrochemical-corrosion behaviors of the coatings in a corrosion environment were analyzed using an electrochemical test, and the corrosion resistance of the coatings was evaluated. The influences of the contents of Al, Zn and Al_2O_3 powder on the structure and electrochemical properties of the coating were studied, and the results provided a theoretical reference for the future research and preparation of new high-quality corrosion-resistant coatings.

2 EXPERIMENTAL PART

2.1 Experimental materials

The substrate material used in the experiment is S135 drill-pipe steel plate, and its chemical composition is shown in **Table 1**. The substrate thickness is 10 mm.

Figure 1 shows the micromorphology of Al and Zn powders. The particles of Zn powders are spherical, ranging from 15–60 μm in size. The particles of Al powders are not uniform; most of them are striplike or wormlike, ranging from 20–60 μm in size. The particles of Al_2O_3 are irregular, ranging from 20–60 μm in size. The purity of the three kinds of powder is more than 99.9 %.

2.2 Preparation of a spray coating

In order to improve mechanical occlusion between the coating and metal substrate, acetone and alcohol were used for ultrasonic cleaning, removing stains and rust from the substrate surface before spraying. The sandblasting pretreatment with quartz sand was used to increase the roughness of the substrate surface, which was beneficial for the bonding between the coating-material particles and substrate. Nine kinds of Al-composite coatings were prepared, and the coating compositions are shown in **Table 2**. The working gas was N_2, the spray-gas pressure was 0.8 MPa and the powder feeding rate was 0.556–1.389 g/s. The spraying temperature was 500 °C. The distance between the spray gun and the surface of the substrate was maintained at 15–30 mm, and the lateral movement was kept at a speed of 20–30 mm/s.

2.3 Performance-characterization methods

The microstructures of the powder and coatings were observed with a ZEISS EV0 MA15 scanning electron microscope (SEM), and the actual thickness of the coatings was measured with a Nikon Eclipse MA100 metallographic microscope. The porosity of each coating (10 different fields of view) was calculated by the M180-50120 metallographic-examination software system, and the average value was obtained. The hardness of the coating was measured with a HXD-1000TMB microhardness tester. The load was 300 gf and the holding time was 10 s. A MFT-4000 multi-functional surface-performance testing machine was used to carry out reciprocating friction tests on different coated sample surfaces under the same loading force, friction frequency, friction length and friction time. Coating phases

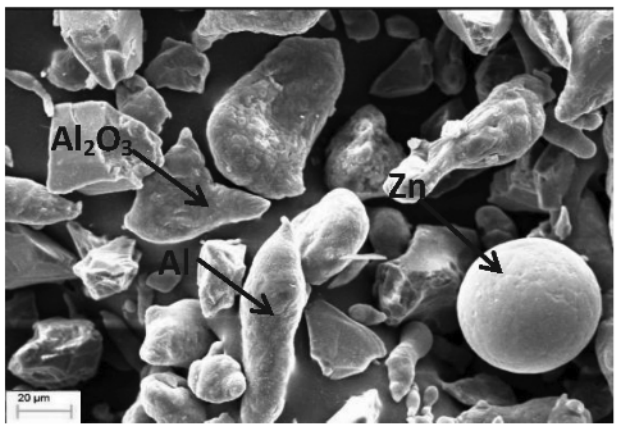

Figure 1: SEM image of mixed powders

were analyzed with a DX-2700 X-ray diffractometer (XRD). The polarization curve was obtained using an AUTOLAB PGSTAT302N electrochemical workstation in a 3.5 % NaCl solution. The applied polarization-potential range was –0.41–0.1 V and the scanning rate was 0.005 mV/s.

3 RESULTS AND DISCUSSIONS

3.1 Microstructure observation of the coatings and porosity

In general, the deformation degree of particles is closely related to the deposition efficiency of particles and the quality of coating. The more severe the deformation, the better is the compactness of the prepared coating and the lower is the porosity. The continuous impact of subsequent particles in a spraying process plays a certain role in the compaction of deposited particles to a certain extent. **Figure 2** shows the micromorphology of the coatings with different powder ratios observed with scanning electron microscopy. It can be seen in **Figures 2a** to **2c** that the surface of the Al-Zn coatings was uneven and there were some round particles with a diameter of about 5 μm. Most of the powder particles underwent severe plastic deformation, while a few of the small particles were not fully deposited due to their impact velocity, not reaching the critical velocity, so there were a few particle gaps or holes on the coating surface.[18] With an increase in the relative content of aluminum powder particles, the roughness of the coating decreased, the porosity of the coating surface decreased gradually, and the coating became more compact. Because the particle size of the Al metal powder was larger than that of the Zn metal powder and irregular, the kinetic energy of the Al powder particles impacting the substrate was larger in the gas-solid two-phase flow field during spraying. As the Al powder particles were continuously impacting the substrate, crystal blocks were broken, refined and mostly flat, so the deformation became obvious.[19]

It can be seen in **Figures 2d** to **2f** that there were a few pits in the coating. Due to the compaction of hard phase Al_2O_3, the coating was generally uniform and dense. The Al particles exhibited obvious plastic deformation and were closely combined in layers in the form of a mutual accumulation, while the Al_2O_3 particles showed no obvious deformation and were embedded in the other particles distributed in the coating. With a decrease in the Al content, the accumulation effect of the

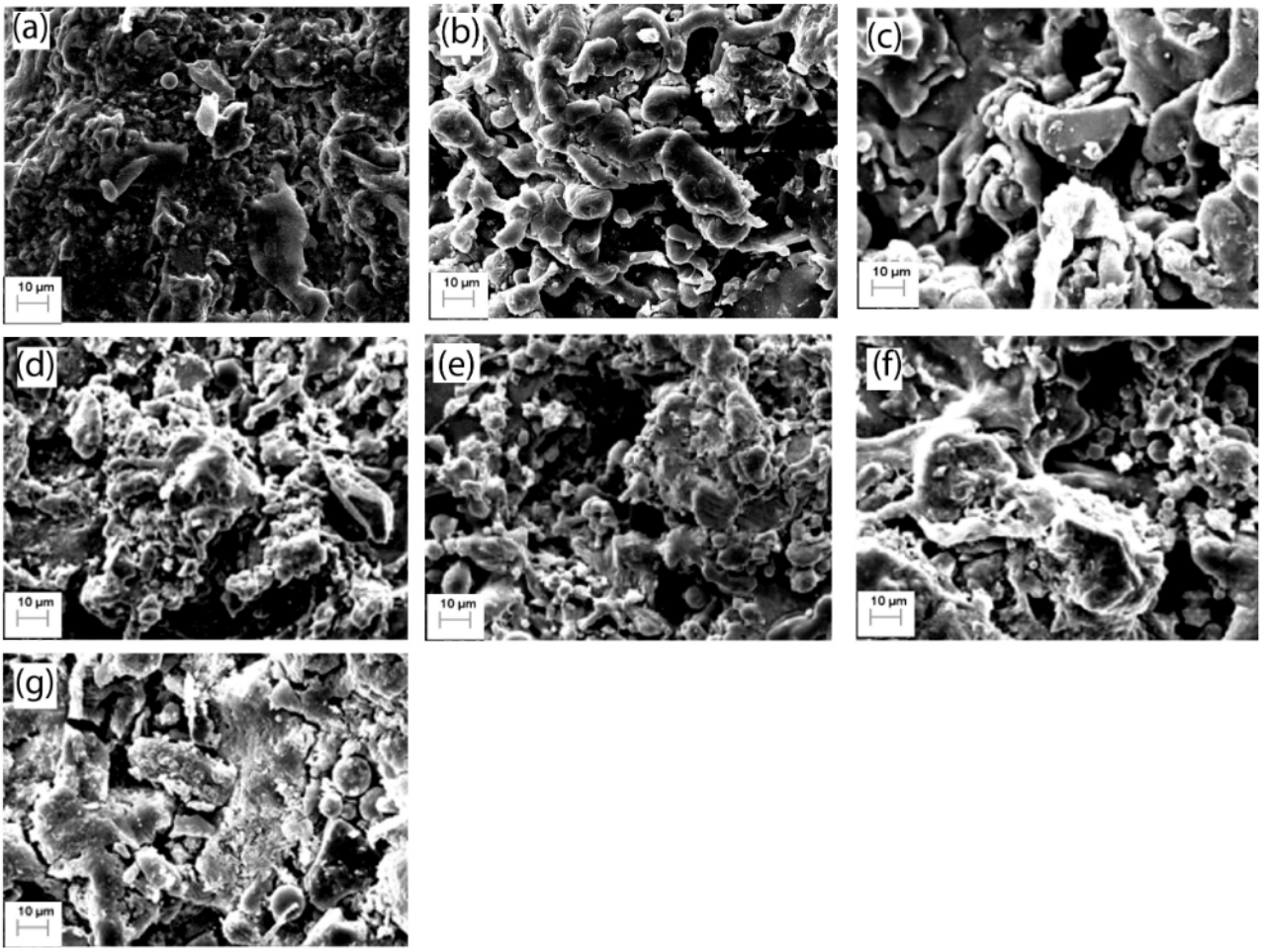

Figure 2: Surface micromorphology of different coatings

Al phase in the coating worsened. With an increase in the Al_2O_3 particles, the porosity of the coating decreased.

It can be seen in **Figures 2g** to **2i** that the coatings were more even and flat on the whole. Zn powder particles were brittle at a certain temperature. They were easily broken into fine particles and deposited in the process of coating preparation, making the coating more compact and greatly reducing the voids caused by overlapping particles, thus reducing the porosity and roughness of the coating. There were a few spherical Zn particles in the coating, mainly due to the facts that the density of the Al powder is much lower than that of the Zn powder and the mass of the Al powder with the same volume is far smaller than that of the Zn powder. The acceleration of the Zn powder was relatively difficult to achieve, and a few particles with a larger particle size failed to reach the critical speed during the acceleration, leading to the failure of effective deposition on the coating surface.

Porosity directly affects the performance of coatings. When coatings are used for corrosion resistance, the value of porosity is the key index to measure the quality of coatings. When the porosity is high, the corrosion rate of the coating accelerates and the corrosive medium can easily enter the coating or intensifies the corrosion of the substrate interface, leading to a decrease in the corrosion resistance of the coating. The porosity of the coatings was calculated with the aid of the image-processing method.[20] Using the M180-50120 metallographic-examination software system, the porosity of the coating was evaluated automatically by "calculating the distribution and size of porosity". The gray value of the metallographic photograph was analyzed with the gray-value method in the metallographic-examination software system to capture the position and size of the pores and determine the porosity of the coating.

The porosity of the nine coatings is shown in **Figure 3**. It can be seen on the figure that the porosity of the nine coatings was less than 1.52 %. Among the first three groups of the Al-Zn coatings, the porosity of Al-80Zn was the largest. With a decrease in the Zn content, the porosity of the coating decreased gradually. When the metal powder particles impacted the S135 steel substrate during spraying, both of them underwent a plastic deformation, making the surface of the substrate develop pits so that the coating powder was trapped in the pits and formed mechanical bonds. With an increase in the Al content in the powder, a lot of Al particles easily accelerated in the gas-solid two-phase flow field. The deposition efficiency of the whole coating increased and large kinetic energy was created, generating sufficient plastic deformation. In addition, due to the continuous impact of the powder particles, the brittle Zn particles became broken and refined, greatly reducing the incomplete overlap between the particles and reducing the porosity.

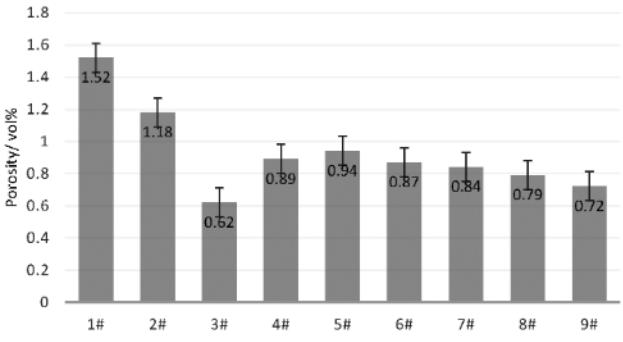

Figure 3: Porosity variation of the coatings

In the middle group including Al-Al_2O_3 coatings, the porosity of the coatings did not change obviously after the Al_2O_3 powder was added. In the last group including Al-Zn-Al_2O_3 coatings, the porosity of the Al-25Zn-20Al_2O_3 coating was only 0.72 %, which showed that the addition of Al_2O_3 to the Al-Zn coating was beneficial as it reduced the porosity. The results showed that the compaction of Al_2O_3 was beneficial to the deposition and densification of the coatings. The porosity of the Al-60Zn coating was the lowest, 0.62 %. The deposition effect of the Al and Zn powder was good, and the deformation of the two types of particles was sufficient. Compared with the Al-60Zn-10Al_2O_3 coating, the porosity of the Al-25Zn-20Al_2O_3 coating was significantly reduced, indicating that the porosity of the coating decreased with an increase in the amount of the Al_2O_3 powder. This indicated that the porosity of the nine types of cold-spray coatings produced in this experiment was lower than that of a thermal-spray coating, whose porosity is usually 5–15 %.[21,22]

3.2 Physical properties of cold-sprayed Al-composite coatings

3.2.1 Coating thickness

The thickness of the nine kinds of coatings was measured with the Nikon Eclipse MA100 metallographic microscope. Eight points were randomly selected for the coating on the cross-section of a sample, and the average value was taken. The results are shown in **Table 3**.

It can be seen from the table below that the thickness of the nine kinds of coatings prepared in this experiment was always over 320 μm, thus providing the basic protection for the substrate. The thickness of the Al-30Al_2O_3 coating was more than 780 μm. The hardness of the hard-phase Al_2O_3 particles was relatively high and there was almost no plastic deformation in the deposition process, which can promote the deposition of the coating to a certain extent. Compared with the Al-30Al_2O_3 coating, the thickness of the Al-Zn coatings was obviously lower. The main reason for this is the fact that under the same process parameters, the fluidity of the Zn powder is poor, and it is easily attached to the inner wall of a nozzle. The increase in the proportion of the Zn powder affected the deposition efficiency of the coating to a certain extent, and the thickness of the coating was also limited. Com-

paring the thickness values for the Al-Al_2O_3 coatings, it can be seen that the addition of Al_2O_3 is beneficial to the deposition of powders to a certain extent.

Table 3: Thickness of the nine Al-composite coatings (μm)

	Coating Number								
	1#	2#	3#	4#	5#	6#	7#	8#	9#
Coating thickness (μm)	327	346	367	751	762	789	635	654	678

3.2.2 Hardness of the coatings

The coating hardness is the key index for evaluating the quality of coatings, and it can reflect the wear resistance of coatings. When the particle velocity reaches the critical velocity, severe plastic deformation will occur after the particle hits the substrate, and then the coating will be deposited. In addition, some particles whose velocity is below critical velocity will produce a shot-peening strengthening effect on the deposited coatings, resulting in the deformation-hardening effect in the coatings.

Figure 4 shows the average hardness values of the nine kinds of coatings. The load of the Vickers microhardness measurements was 300 gf. Eight different positions of the coating on each cross-section of a sample were randomly selected for the measurement and then the average value was calculated. Under the action of high-speed and high-pressure gas, fully solidified high-speed particles violently collided with the substrate. The subsequent spray particles had a certain shot-peening strengthening effect on the deposited coating and there was a certain deformation-hardening effect in the coating. Literature[23] shows that the particles in the spraying process undergo cold forging, while a continuous work-hardening effect and compressive stress of a coating help to improve its hardness.

The hardness of all the nine coatings was higher than 37 HV 0.3. As the hardness of the Zn-powder particles was much higher than that of the Al-powder particles under the same working parameters during the spraying, for the first group consisting of the Al-Zn coatings, the hardness of the coatings increased with the increase in the content of the Zn-powder particles. The hardness of the coating was significantly improved with the addition of hard-phase Al_2O_3 particles because the hardness of the Al_2O_3 particles was relatively high. At the same time, the continuous impact of the Al_2O_3 particles played a significant role in the compaction, and the work-hardening effect was relatively obvious. In the middle group consisting of the Al-Al_2O_3 coatings, the hardness of the coatings increased with the increase in the content of the Al_2O_3 particles, and the hardness of the three coatings was higher than 45 HV 0.3. In the last group consisting of the Al-Zn-Al_2O_3 coatings, the hardness of the three coatings was generally higher than 51 HV 0.3, and that of the Al-25Zn-20Al_2O_3 coating was more than 62 HV 0.3.

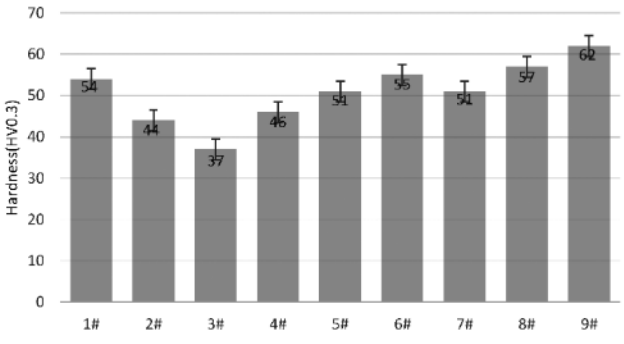

Figure 4: Hardness of the coatings

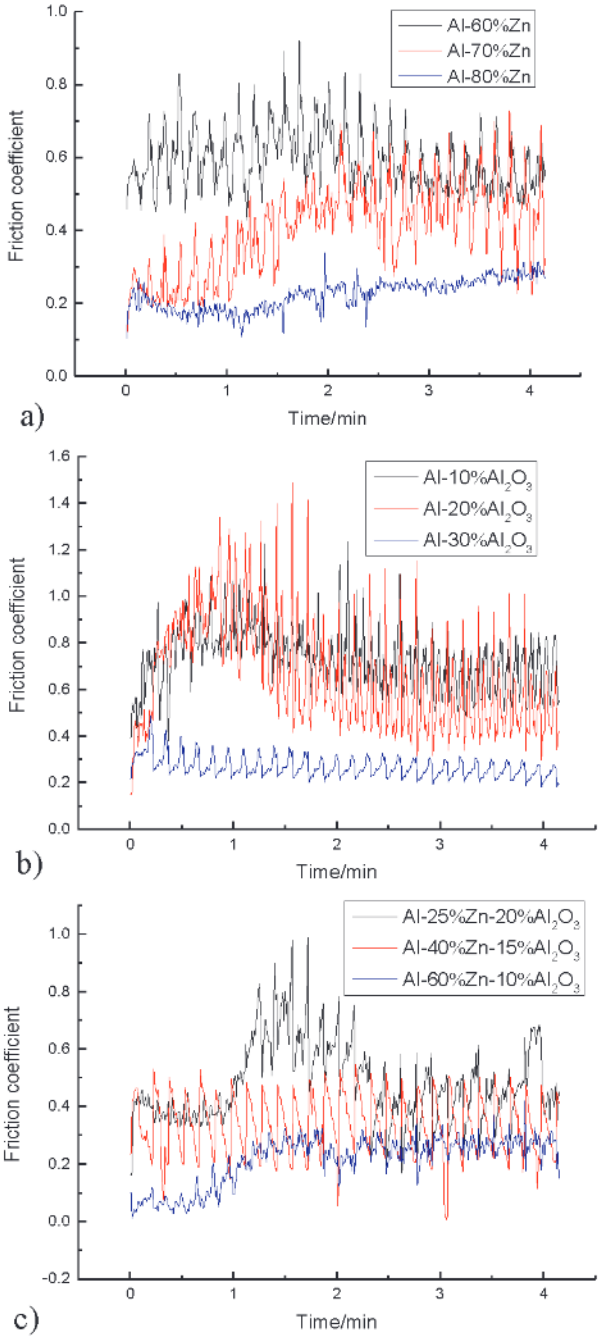

Figure 5: Relationship between friction coefficient and time for the coatings

3.2.3 Friction property of the coatings

Under the actual working condition, due to the friction of the well wall or casing wall, the surface of a drill-pipe joint is required to have a certain wear resistance. The friction coefficient and wear resistance of a coating are important indexes for evaluating the wear resistance of the coating. Firstly, the friction coefficient of a composite coating with different mass fractions is measured with a reciprocating-friction test so as to determine the wear resistance and wear mechanism of the composite coating. The characterization of the wear resistance of the composite coating was mainly determined using a reciprocating-friction test with the help of a multifunctional material-surface performance tester (MFT-4000). Under the condition of a load force of 10 N, friction length of 10 mm, test time of 10 min and friction frequency of 50 mm/min, the reciprocating-friction test was carried out on the nine kinds of coating surfaces.

The obtained change curve of the friction coefficient with time is shown in **Figure 5**. As can be seen in **Figure 5a**, the friction coefficients of three coatings follow each other in the following order: Al-60Zn, Al-70Zn, Al-80Zn. As the hardness of Zn particles was higher than that of Al, the hardness of the coating increased with the increase in the Zn content and the friction coefficient decreased. It can be seen from **Figure 5b** that the friction coefficient of three coatings decreased with the increase in the Al_2O_3 powder content because the Al_2O_3 material itself has high hardness and wear resistance, producing a self-lubricating effect when subjected to an external force.[24] It can be seen from **Figure 5c** that the friction coefficients of the Al-Zn-Al_2O_3 coatings were generally low, and that of the Al-60Zn-10Al_2O_3 coating was the lowest.

3.3 Corrosion behavior of coatings

Metal corrosion refers to the phenomenon of damage or failure caused by the interaction between metal materials and a medium in its environment. In order to evaluate the corrosion resistance of the coatings, immersion tests were carried out on the coating samples. 10 % NaCl solution was chosen as the corrosion solution for the immersion-corrosion experiment. As a kind of anode coating, the Al coating not only had the function of isolating the corrosion medium and making it unable to react with the substrate, but was also a kind of a sacrificial anode material, which played a role in the cathodic protection.

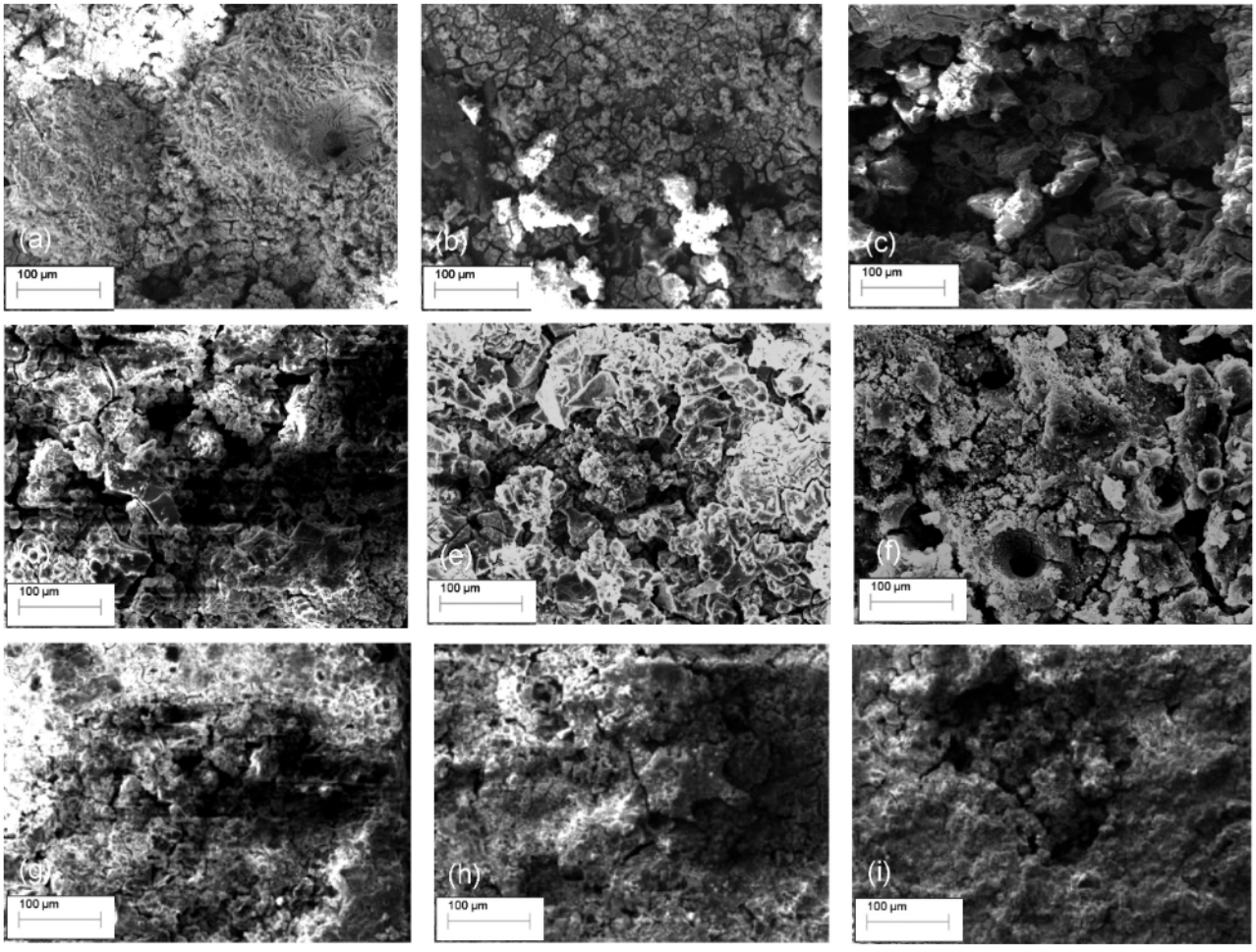

Figure 6: SEM micrographs of the surface morphology of the coatings after corrosion

Zn coating is often used as the sacrificial anode to protect steel. The Al-Zn composite coating had both advantages. The morphology of the coating was observed after 480 h. By observing the corrosion surface morphology of the coatings after immersion corrosion, it was found that a layer of white dense corrosion products was deposited on the coating surface.

The surface morphology of the coatings after corrosion is shown in **Figure 6**. From **Figures 6a** to **6c**, it can be seen that a few holes and island particles appeared on the surface of the Al-Zn coatings. The distribution of corrosion products was uneven and there were obvious corrosion pits and agglomerations of corrosion products around the corrosion pits. Zn was dissolved on the surface of the coatings, the microcracks in the coatings expanded and the surface of the coatings contained acicular corrosion products, which indicated that the corrosion resistance of the coating was low. It can be seen from **Figures 6d** to **6f** that there were many network corrosion cracks on the surface of the Al-Al_2O_3 coating and large holes in the coating and the number and size of the holes inside the Al_2O_3 layer increased obviously. From **Figures 6g** to **6i**, it can be seen that the density of corrosion products on the coating surface increased with the increase in the Al and Al_2O_3 content. When the content of Al was relatively low, Zn was relatively active and was the first to corrode, forming a cathodic-protection effect on Al. Due to the decrease in the porosity of the Al-Zn-Al_2O_3 coating, the corrosion products were dense and there was no obvious porosity. The denser the corrosion product, the more it can prevent the coating from being corroded.

The samples were weighed before and after corrosion, and the average annual corrosion rate was calculated based on the corrosion weight loss of the measured samples. The calculation formula is as follows:

$$V_a = C \times \frac{W_0 - W}{\rho A t} \quad (1)$$

where V_a is the annual corrosion rate, C is the conversion factor and its value is 8.76×10^4; W_0 is the quality of the samples before corrosion, W is the quality of the samples after corrosion, A is the surface area of the samples, ρ is the density of the coating surface, t is the corrosion time.

In accordance with Equation (1), the corrosion rate of each coating is shown in **Figure 7**. The annual corrosion rate of the Al-Zn coatings decreased with the decrease in the Zn content. The annual corrosion rate of the Al-Al_2O_3 coatings decreased with the increase in the Al_2O_3 content. The annual corrosion rate of the Al-Zn-Al_2O_3 coatings decreased with the increase in the Al and Al_2O_3 content.

Figure 8 shows the XRD composition of the nine coatings after corrosion. As can be seen from **Figure 8a**,

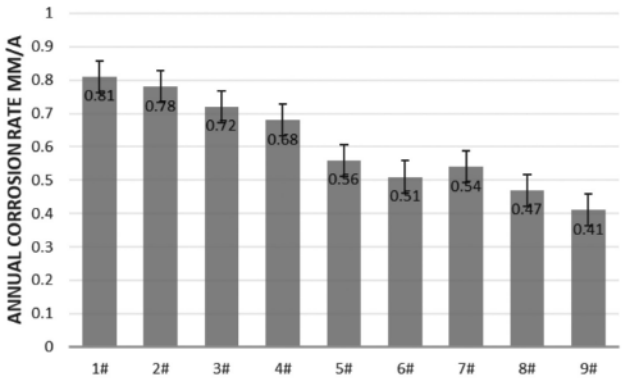

Figure 7: Corrosion rate of each coating

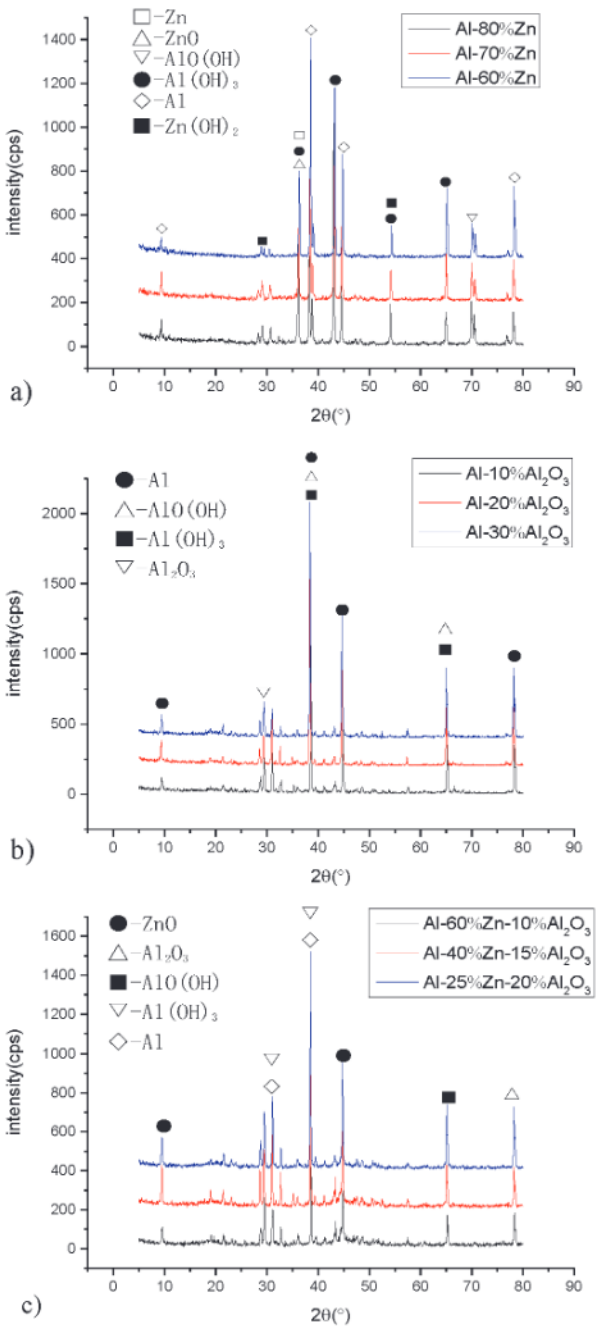

Figure 8: XRD diagrams of three coatings after corrosion

the corrosion products of Al-Zn coatings contain AlO(OH), $Al(OH)_3$, ZnO and Al_2O_3. A passivation film was easily formed by the oxidation of Al in an aqueous solution. The anode first underwent the anodic dissolution reaction of Al. With the corrosion reaction, the passive film on the coating surface was destroyed and the corrosion reaction of the coating was intensified. In the subsequent corrosion process, because Zn was more active than the oxide film of Al, it could protect the oxide film of Al. With the continuous dissolution of Zn and the formation of $ZnO{\cdot}H_2O$ with the OH^- generated from the cathode, the product covered the coating surface.

These corrosion products can play a role in "self-sealing" plugging of the pores to some extent, blocking the penetration and diffusion of the medium into the coating.[14] It can be seen from **Figure 8b** that, in addition to the unreacted Al and $Al(OH)_3$ formed due to the reaction of Al with OH^- in water, AlO(OH) was also formed, exhibiting high hardness and compactness so that it could hinder the subsequent corrosion reaction. Therefore, the higher the Al_2O_3 content, the smaller was the corrosion rate. It can be seen from **Figure 8c** that Al was the most active in the coating sample, and the reaction products included $Al(OH)_3$ and AlO(OH), which can effectively protect the substrate from contacting the corrosive medium as the passivating agent. The activity of Zn was higher than that of the Al oxide film, which provided protection for the Al oxide film to some extent. The corrosion reaction of Zn took place and ZnO was formed.

Polarization curves of the nine coatings and substrate in the 3.5 % NaCl solution are shown in **Figure 9**. There was no obvious passivation zone during the polarization of the nine coatings. The corrosion potential of the nine coatings was lower than that of the substrate. The corrosion rate of the nine coatings in the 3.5 % NaCl solution was lower than that of the substrate. With the increase in the content of the Al powder in the metal powder, the corrosion potential of the coating increased and the corrosion rate of the coating decreased. The corrosion potential of the Al-Al_2O_3 coatings was relatively high, about 0.88 V. The corrosion potentials of the other cold-sprayed Al-Zn coatings and Al-Zn-Al_2O_3 coatings were about –1.0 V to –1.06 V. The potential of the nine cold-sprayed coatings was much lower than that of the S135 steel, providing good protection of the steel substrate. The current density was higher than that of the substrate, and the corrosion could occur rapidly to protect the steel substrate.

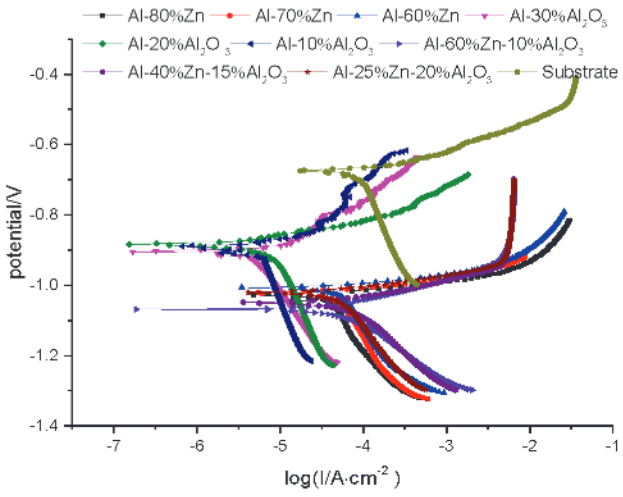

Figure 9: Polarization curves of three coatings in the 3.5% NaCl solution

4 CONCLUSIONS

There were no obvious defects on the surface of the nine kinds of Al composite coating. The coating surface was relatively even and flat, the particle plastic deformation was sufficient and the density was high. An addition of the Al_2O_3 powder can improve the adhesion of a coating, and an addition of the Zn powder can make it more compact.

The porosity of the nine coatings was less than 1.52 %. The porosity of the Al-60Zn coating was only 0.62 %. A proper increase in the amount of the Zn powder was beneficial for the reduction of the porosity of the coating. The porosity of the Al-Zn-Al_2O_3 coating decreased obviously after adding Al_2O_3 powder.

The Al-Al_2O_3 coating was easily deposited and its thickness was more than 750 μm, while the thickness of the other eight coatings was more than 320 μm. The thickness of the coating can be increased with an increase in the Al_2O_3 and Zn powder amounts. The hardness of the nine coatings was above 37 HV 0.3 and the hardness of the Al-25Zn-20Al_2O_3 coating was above 62 HV 0.3. The hardness of the coating with the Al_2O_3 powder was obviously higher than that of most of the other coatings without the Al_2O_3 powder. The friction coefficient of the coatings decreased with the increase in the Zn and Al_2O_3 content.

The potential of the nine cold-sprayed coatings was much lower than that of the S135 steel. The current density was higher than that of the substrate and the corrosion could occur rapidly to protect the steel substrate. The corrosion rate of the coatings decreased with the increase in the contents of Al and Al_2O_3. The density of corrosion products on the surface of a coating increased with the increase in the contents of Al and Al_2O_3. The denser the corrosion products, the better the coating can be prevented from corrosion.

Acknowledgments

The authors would like to acknowledge the funding support from the Chinese National Natural Science Foundation (51974271) and Innovation Fund for Key Laboratory of natural gas development and utilization of

new materials (Southwest Petroleum University) (Grant no. X151519KCL19).

5 REFERENCES

[1] L. Fang-Po, H. Li-Hong, L. Yong-Gang, W. Yong, Investigation on toughness index of high grade steel drill pipe, Journal of China University of Petroleum (Edition of Natural Science), 35 (**2011**) 5, 130–133

[2] L. Jian-Jun, Z. Jun-Jie, Study on fracture characteristics of S135 steel for drill pipes, Foundry Technology, 36 (**2015**) 10, 2477–2478

[3] K. A. Macdonald, J. V. Bjune, Failure analysis of drillstrings, Engineering Failure Analysis, 30 (**2007**) 14, 1641–1666, doi:10.1016/j.engfailanal.2006.11.073

[4] S. Moradi, K. Ranjbar, Experimental and computational failure analysis of drillstrings, Engineering Failure Analysis, 32 (**2009**) 16, 923–933, doi:10.1016/j.engfailanal.2008.08.019

[5] S. A. Mikaeva, A. S. Mikaeva, Protective Coatings, Glass and Ceramics, 74 (**2017**), 144–146, doi:10.1007/s10717-017-9949-5

[6] R. Fernandez, B. Jodoin, Cold Spray Aluminum–Alumina Cermet Coatings: Effect of Alumina Morphology, J. Therm. Spray Tech., 28 (**2019**), 737–755, doi:10.1007/s11666-019-00845-5

[7] L. Fan, F. Tang, G. Chen, S. T. Reis, M. L. Koenigstein, Corrosion Resistances of Steel Pipe Coated with Two Types of Enamel by Two Coating Processes, Journal of Materials Engineering and Performance, 27 (**2018**) 10, 5341–5349, doi:10.1007/s11665-018-3656-4

[8] R. Nikbakht, S. H. Seyedein, S. Kheirandish, H. Assadi, B. Jodoin, The role of deposition sequence in cold spraying of dissimilar materials, Surface and Coatings Technology, 367 (**2019**), 75–85, doi:10.1016/j.surfcoat.2019.03.065

[9] China National Defense Science and Technology Information Center, World Weapons and Equipment and Military Technology Annual Development Report 2014, 2015, 903–904

[10] L. Wenya, Y. Kang, Y. Shuo, Y. Xiawei, X. Yaxin, R. Lupoi, Solid-state additive manufacturing and repairing by cold spraying: A review, Journal of Materials Science & Technology, 34 (**2018**), 440–457, doi:CNKI:SUN:CLKJ.0.2018-03-004

[11] Z. Guo-feng, W. Ying-ying, Z. Hai-long, T. Jun-lei, C. Yong-dong, Application of Cold Spraying Equipment and Cold Spraying Technology, Surface Technology, 46 (**2017**) 11, 198–205

[12] S. Siddique, A. A. Bernussi, S. Wilayat Husain, M. Yasir, Enhancing structural integrity, corrosion resistance and wear properties of Mg alloy by heat treated cold sprayed Al coating, Surface and Coatings Technology, 394 (**2020**) 7, 125882, doi:10.1016/j.surfcoat.2020.125882

[13] W. Xiujin, Z. Liuyan, Z. Xiaolan, W. Wei, J. Xiaohua, Corrosion behavior of Al_2O_3-reinforced graphene encapsulated Al composite coating fabricated by low pressure cold spraying, Surface and Coatings Technology, 386 (**2020**), 125486, doi:10.1016/j.surfcoat.2020.125486

[14] C. Walde, D. Cote, V. Champagne, R. Sisson, Characterizing the effect of thermal processing on feedstock Al alloy powder for additive manufacturing applications, Journal of Materials Engineering and Performance, 28 (**2018**), 601–610, doi:10.1007/s11665-018-3550-0

[15] N. Sieglind, N. Tungwai, V. Florian, W. Story, L. N. Brewer, Saltwater corrosion behavior of cold sprayed AA7075 aluminum alloy coatings, Corrosion Science, 130 (**2018**), 231–240, doi:10.1016/j.corsci.2017.10.033

[16] I. Eric, L. Jean-Gabriel, A. Bernard, M. Christian, Investigation of Al-Al_2O_3 cold spray coating formation and properties, Journal of Thermal Spray Technology, 16 (**2009**), 661-668

[17] J. Martin, K. Akoda, V. Ntomprougkidis, O. Ferry, Duplex surface treatment of metallic alloys combining cold-spray and plasma electrolytic oxidation technologies, Surface and Coatings Technology, 392 (**2020**), 125756, doi:10.1016/j.surfcoat.2020.125756

[18] F. Raletz, M. Vardelle, G. Ezo'o, Critical particle velocity under cold spray conditions, Surface and Coatings Technology, 201 (**2006**) 5, 1942–1947, doi:10.1016/j.surfcoat.2006.04.061

[19] X. Qiu, Naeem ul Haq Tariq, Microstructure, microhardness and tribological behavior of Al_2O_3 reinforced A380 aluminum alloy composite coatings prepared by cold spray technique, Surface and Coatings Technology, 350 (**2018**) 9, 391–400, doi:10.1016/j.surfcoat.2018.07.039

[20] D. Lv, Z. Lian, T. Zhang, Study of cavitation and cavitation erosion quantitative method based on image processing technique, Advances in Civil Engineering, 2018, 5317578, doi:10.1155/2018/5317578

[21] Jo Ann Gan, C. C. Berndt, Effects of standoff distance on porosity, phase distribution and mechanical properties of plasma sprayed Nd-Fe-B coatings, Surface and Coatings Technology, 216 (**2016**), 127–138, doi:10.1016/j.surfcoat.2012.11.040

[22] G. A. Baglyuk, S. G. Pyatachuk, A. A. Mamonova, The structure and properties of boride coatings depending on the porosity of powder steel preforms, Powder Metallurgy and Metal Ceramics, 53 (**2014**), 417–422, doi:10.1007/s11106-014-9633-z

[23] R. C. Dykhuizen, M. F. Smith, D. L. Gilmore, et al., Impact of High Velocity Cold Spray Particles, Journal of Thermal Spray Technology, 8 (**1999**) 4, 559–564, doi:10.1361/105996399770350250

[24] D. Jun, W. Hong-mei, W. Xin, Analysis of Influencing Factors on Critical Load of Adhesion Strength in Scratch Test, Surface Technology, 44 (**2015**) 09, 134–139

Data Availability

The data used to support the findings of this study are available from the corresponding author upon request. I would like to declare, on behalf of my co-authors, that the work described is original research that was not published previously, and is not under consideration for publication elsewhere, in whole or in part. All the authors listed have approved the manuscript.